

Short vs. Long-term Coordination of Drones: When Distributed Optimization Meets Deep Reinforcement Learning

Chuhao Qin*, and Evangelos Pournaras*

*School of Computing, University of Leeds, Leeds, UK

Abstract—Swarms of autonomous interactive drones, with the support of recharging technology, can provide compelling sensing capabilities in Smart Cities, such as traffic monitoring and disaster response. This paper aims to deliver a novel coordination solution for the cost-effective navigation, sensing, and recharging of drones. Existing approaches, such as deep reinforcement learning (DRL), offer long-term adaptability, but lack energy efficiency, resilience, and flexibility in dynamic environments. Therefore, this paper proposes a novel approach where each drone independently determines its flying direction and recharging place using DRL, while adapting navigation and sensing through distributed optimization, which improves energy-efficiency during sensing tasks. Furthermore, drones efficiently exchange information while retaining decision-making autonomy via a structured tree communication model. Extensive experimentation with datasets generated from realistic urban mobility underscores an outstanding performance of the proposed solution compared to state-of-the-art methods. Significant new insights show that long-term methods optimize scarce drone resource for traffic management, while the integration of short-term methods is crucial for advising on charging policies and maintaining battery safety.

Index Terms—drones, UAV, navigation, sensing, charging, distributed optimization, deep reinforcement learning

I. INTRODUCTION

Unmanned Aerial Vehicles (UAVs), referred to as drones, can organize themselves into swarms, fostering collaboration and efficiency in sensor data collection within Smart Cities [1]. With their mobility, autonomy, and diverse sensors, drones have been widely used in several applications, such as reporting traffic congestion at early stage [2], and mapping natural disasters [3]. However, the inherent limitations in battery capacity of drones influence their spatio-temporal coverage. On the other hand, it requires a high cost to build and maintain a large-scale drone swarm together. Therefore, efficient resource management is essential for long operations of drones by ensuring optimal drone recycling and preventing battery depletion. Recently, scholars have introduced the recharging technologies and commercially wireless charging stations for long-term sensing [4].

Inspired by these studies, this work tackles the problem of coordinating swarms of drones for improved distributed navigation, sensing and recharging. The goal is to enhance sensing quality in a large-scale area using both drones and charging stations while minimizing the overall involved costs.

This endeavor requires highly adaptive and optimized drone operations. Previous work [5] employs distributed optimization methods for efficient drones path planning and task assignment to enhance sensing quality. These methods enable drones to autonomously self-organize and self-assign their tasks collectively, while respecting privacy and autonomy of drones. However, these methods are reactive to the current state of the environment rather than proactive to address long-term operational challenges strategically. The navigation and sensing of drones are significantly influenced by two factors: their flying directions and future requirements for sensor data on the map. For example, drones equipped with insights about the expected increase in traffic flow in certain areas can proactively fly to those locations, even if vehicle density is currently low. This strategic decision can be more effective to allocate limited drone resources for tasks like vehicle detection, although in short-term the benefits are not evident. This underscores the "slower is faster" effect, highlighting the need for long-term planning to optimize overall effectiveness and efficiency in drone sensing operations.

Deep reinforcement learning (DRL) tackles the challenge of long-term optimization. It accounts for long-term and iterative actions through the Bellman equation, which considers the discounted cumulative reward of agents' actions [6], [7]. Drones, as heterogeneous agents with distinct behavior patterns and action spaces, can benefit from the powerful deep neural networks employed in DRL, enabling an effective handling of sophisticated state space and time-varying environments. Nevertheless, as the number of drones and time periods increase, the curse of dimensionality constrains efficient sensing. For instance, considering a scenario where drones are tasked with learning optimal path planning over a broad range of time scales using DRL. In this setting, the high number of epochs may inadvertently compel the drones to take unnecessary actions. As a result, drones could choose longer paths, leading to higher energy consumption. Furthermore, current methods overlook the need for drones to become more flexible and adaptive to real-time environmental changes while maintaining system resilience, against single points of failure. Addressing these limitations requires reducing actions in a temporal scale as well as effective autonomous mission planning distributively, but no existing approaches incorporate these novelties.

Therefore, in this paper, we propose a new approach for the coordination of swarms of drones, *Distributed Optimization and (deep) Reinforcement Learning (DO-RL)*, which involves

a novel multi-agent DRL algorithm that builds upon on a collective learning approach [8], [9]. *DO-RL* relies on a learning model to determine the drones' strategic navigation and flying directions for sensing, which also determines the recharging stations, while leaving the self-planning and selection of specific sensing operations to distributed optimization, i.e., collective learning. This approach significantly reduces the number of decisions in a temporal scale, avoiding unnecessary energy consumption. Then, we design a structured tree communication model within which each agent interacts with its children and parent in a bottom-up and top-down fashion, obtains the aggregated observation to calculate immediate reward in DRL, and independently decides its navigation and sensing. This ensures scalability (support of a large number of agents), efficiency (low communication and computational cost), decentralization and resilience [10]–[12]. Furthermore, a set of auxiliary approaches is introduced, including a plan generation strategy that provides high-quality and diverse options for drones navigation and sensing, a plan selection, a periodic state update and a centralized training and decentralized execution framework. To evaluate the effectiveness of *DO-RL*, this paper conducts experimental evaluations with real-world data and emulated traffic monitoring scenarios, comparing it against state-of-the-art baseline methods.

The contributions of this paper are outlined as follows: (i) The first attempt to coordinate navigation, sensing, and recharging by a swarm of autonomous and self-planning drones in a distributed and cost-effective way. (ii) A novel approach, *DO-RL*, to address this problem using both multi-agent DRL and distributed optimization. (iii) The applicability of a designed structured tree communication model for efficient planning and information sharing among agents to ensure decentralization, resilience, and flexibility. (iv) A testbed for extensive experimentation with realistic traffic patterns and real-world transport networks. (v) The validation for the superior performance of the proposed approach over three state-of-the-art methods. (vi) An open-source implementation of the proposed approach and an open dataset [13] containing all plans of the studied scenario. They can be used as benchmarks to encourage further research on this problem.

TABLE I
COMPARISON TO RELATED WORK: CRITERIA COVERED (✓) OR NOT (✗).

Criteria	Ref.:	[14]	[15]	[16]	[17]	[18]	[19]	[20]	This paper
Decentralization		✓	✓	✓	✗	✓	✗	✗	✓
Long-term efficiency		✗	✗	✗	✓	✓	✓	✓	✓
Recharging assignment		✗	✗	✗	✗	✗	✓	✗	✓
Scalability		✗	✗	✓	✗	✗	✗	✗	✓
Resilience		✗	✗	✓	✗	✗	✗	✗	✓
Flexibility		✓	✓	✓	✗	✗	✗	✗	✓

II. RELATED WORK

Sensing task assignment. The UAV task assignment problem for spatio-temporal sensing has been traditionally defined as a combinatorial optimization problem, resembling the Traveling Salesmen Problem [5]. This involves finding the optimal assignment of tasks to drones at specific locations, while

considering constraints such as task urgency, time scheduling, and flying costs. The digraph-based methods, such as greedy approach, [21], ant colony optimization [22], and genetic algorithm [23], are introduced to formulate the problem of reaching optimal sensing efficiency in terms of coverage, inspection delay, events detection rate and the cost of flying trajectories. However, these works lack comprehensive evaluation in complex sensing scenarios, such as varying time periods, charging stations, and different sensing distributions. Moreover, these centralized methods suffer from a risk of single points of failure [24], wherein the failure of a central control station can lead to several system disruptions without autonomous recovery mechanisms.

Distributed optimization. Several distributed task assignment algorithms have been proposed to address the challenges of multi-UAV systems in complex sensing scenarios. One such algorithm is the robust decentralized task assignment (RDTA) [14] that enhances robustness and reduces communication costs by employing decentralized planning for drones. Another algorithm is the consensus-based bundle algorithm (CBBA) [15], which combines market-based mechanisms and situation awareness to converge and avoid task conflicts among drones. Furthermore, a planning-based coordination method using collective learning, named Economic Planning and Optimized Selections (EPOS), enables drones to optimize their navigation and sensing options under battery constraints [16], [25]. However, long-term sensing scenarios pose challenges. Drones tend to prioritize immediate maximum returns in the short term, often overlooking the need for strategic decision-making for decentralized navigation, sensing and recharging.

DRL-based drone sensing. The deep reinforcement learning (DRL) algorithm proves to be effective when addressing the distributed sensing problem with drones using complex optimization objectives, limited energy consumption, and a large number of heterogeneous agents. Afrin *et al.* [26] designed a DRL-based model for edge servers to dynamically allocate tasks to robots (e.g., drones), aimed at enhancing system resilience in smart farming environments. Ding *et al.* [17] integrated the mobile crowdsensing (i.e., human equipped with mobile sensing devices such as smartphones) into UAV sensing, which overcomes the limitations of both human mobility and drone battery capacity. Omoniwa *et al.* [18] presented a decentralized approach that leverages DRL and shared information from neighbors to improve the energy efficiency of drones in providing wireless connectivity to ground users in dynamic environments. Nevertheless, these approaches lack privacy and autonomy for drones in self-assignment tasks, reducing flexibility, adaptability to the real-time environmental changes and increasing vulnerability to single points of failure. Moreover, they are confined to a small number of drones and time periods due to the huge action space. In contrast, our approach empowers agents to determine overall flying directions every time period, leaving specific navigation and sensing tasks in each timeslot to planning and selection. This strategic allocation significantly filters out unnecessary actions and reduces the corresponding energy consumption.

Recharging assignment. Earlier work [27], [28] has studied

the recharging scheduling problem: drones efficiently collect sensor data while charging from stations. However, scalability becomes a challenge since the algorithms used in these works only deal with a small number of drones. Zhao *et al.* [19] proposed a comprehensive solution for sustainable urban-scale sensing in open parking spaces, specifically for detecting available parking spots. Their solution incorporates the task selection and scheduling using DRL, and adaptive charging scheduling. However, this approach is centralized and tailored exclusively to the scenario of open parking spaces.

Transportation application. Despite the potential of drones in improving traffic monitoring accuracy, safety, and cost savings, there is limited research on task assignment in this particular scenario. Elloumi *et al.* [29] proposed a road traffic monitoring system that generates adaptive drones trajectories by extracting information about vehicles. Huang *et al.* [30] developed the pre-flight conflict detection and resolution method, where service providers of drones with their own interest can coordinate to address the path planning problem. Samir *et al.* [20] leveraged a DRL algorithm to optimize the trajectories of UAVs, with the objective of minimizing the age of information of collected data. While these approaches demonstrate high performance in the detection of traffic vehicles, they do not explicitly address the challenges of decentralized sensing and recharging. Furthermore, they assume prior knowledge of the traffic flow of the vehicles, which may not be readily available in practical scenarios.

In summary, this paper bridges a gap in previous approaches. It empowers drones to make strategic choices in flying directions and recharging locations by predicting traffic flow, while enabling them to autonomously optimize their sensing operations, ensuring decentralization, resilience, and flexibility.

III. SYSTEM MODEL

Table II illustrates the list of mathematical notations used in this paper.

A. Scenario and Assumptions

Sensing map. Consider a swarm of drones $\mathcal{U} \triangleq \{1, 2, \dots, U\}$ performing sensing missions, such as monitoring vehicles, over a grid that represents a 2D map. In this scenario, a set of grid cells (or points of interest) $\mathcal{N} \triangleq \{1, 2, \dots, N\}$ are uniformly arranged to cover the map. The primary goal of the drones is to coordinate their visits to these cells to collect the required data. Furthermore, a set of charging stations $\mathcal{M} \triangleq \{1, 2, \dots, M\}$, from which the drones depart from and return to, are located at fixed coordinates on the map.

Time periods and slots. We assume a set of time periods as $\mathcal{T} \triangleq \{1, 2, \dots, T\}$. Each time period can be divided into a set of equal-length scheduling timeslots $\mathcal{S} \triangleq \{1, 2, \dots, S\}$. In each timeslot, a drone can be controlled to fly to a cell and hover to collect sensor data.

Action. To explain the long-term navigation and sensing over all periods, we introduce the period-by-period actions of each drone $a^u = \{0, 1, 2, \dots, 8\}$, $u \in \mathcal{U}$, meaning to control u

TABLE II
NOTATIONS.

Notation	Explanation
u, U, \mathcal{U}	Index of a drone; total number of drones; set of drones
m, M, \mathcal{M}	Index of a charging station; total number of charging stations; set of charging stations
n, N, \mathcal{N}	Index of a grid cell; total number of grid cells; set of grid cells
s, S, \mathcal{S}	Index of a timeslot; total number of timeslots in a period; set of timeslots
t, T, \mathcal{T}	Index of a period; total number of periods; set of periods
a^u	The action or flying direction taken by u
$P^u, p_{n,s}^u$	The plan of u ; value of P^u at cell n and timeslot s
$P^{-u}, p_{n,s}^{-u}$	The observed plans of drones by u excluding P^u ; value of P^{-u} at cell n and timeslot s
$p_{n,s}$	The aggregated plans of all drones at cell n and timeslot s
$V_{n,s}$	Required sensing value at cell n and timeslot s
$v_{n,s}$	Collected sensing value at cell n and timeslot s
$\mathcal{R}, r_{n,s}$	Target; target value at cell n and timeslot s
l, L	Index of a plan in G^{a^u} ; total number of plans in G^{a^u}
$C^f(u), t^f$	Flying power consumption of u ; flying time
$C^h(u), t^h$	Hovering power consumption of u ; hovering time
c^u, e^u	Current location of u ; current energy consumption of u
$K(a^u)$	Indexes of cells within the searching range along flying direction a^u
$J(a^u)$	Indexes of visited cells within $K(a^u)$
β	Behavior of an agent in planning optimization
o_t^u, r_t^u	Observation of u at period t ; reward of u at the period t
k, H	Index of a sampled transition; number of sampled transitions
γ, ϵ	Discount factor; clip interval hyperparameter
$Q(\cdot), \theta^Q$	Critic network; parameter of critic network
$\pi(\cdot), \theta^\pi$	Actor network; parameter of actor network
$\omega_{n,s}, \bar{v}$	Prediction coefficient to calculate $\hat{V}_{n,s}$; threshold to remove the regions with low sensing requirements
I, \mathcal{X}, A	Total number of iterations in EPOS; size of state space; number of actions in DRL
\mathcal{E}, W	Number of episodes; number of neutrals per layer in DNN

to move horizontally along eight directions, which are 1 = north (N), 2 = east (E), 3 = south (S), 4 = west (W), 5 = northeast (NE), 6 = southeast (SE), 7 = southwest (SW), and 8 = northwest (NW), or return to the origin ($a^u = 0$). Under each action, u executes a short-term navigation and sensing. After completing its sensing tasks, u flies back to one of the charging stations to recharge fully and resume work in the next period $t + 1$.

Matrix of plans. To explain the short-term navigation and sensing of drones over the cells and timeslots in a period t , $t \in \mathcal{T}$, the plan of a drone u that travels through the direction of a^u is introduced, denoted by $P^u(a^u, t)$. It represents the specific navigation and sensing details, including the visited cells and corresponding energy consumption. The plan $P^u(a^u, t)$ is encoded by a matrix of size $N \times S$, with each element represented as $p_{n,s}^u(a^u, t) \in \{0, 1\}$. Here, $p_{n,s}^u(a^u, t) = 1$ denotes that the drone u hovers and collects all required data at cell n at timeslot s , whereas for $p_{n,s}^u(a^u, t) = 0$ the drone does not hover at that cell at that time. Moreover, $P^{-u}(a^u, t) = \{p_{n,s}^{-u}(a^u, t) | n \in \mathcal{N}, s \in \mathcal{S}\}$ denotes the observed plans by drone u in time period t , indicating that it incorporates and sums the plans of all other drones excluding its own. We formulate the aggregated plans of all drones observed by u at cell n and timeslot s as follows:

$$p_{n,s}(a^u, t) = p_{n,s}^u(a^u, t) + p_{n,s}^{-u}(a^u, t). \quad (1)$$

Matrix of required sensing values. In the context of a sensing task, each cell at a timeslot has specific sensing requirements that determine the data acquisition goal of drones. Such sensing requirements can be determined by city authorities as a continuous kernel density estimation, for example, monitoring cycling risk based on requirements calculated by past bike accident data and other information [16], [31]. The high risk level of a cell at a timeslot represents the high importance of sensing (e.g., the crucial intersection of traffic flow), and thus a high number of required sensing values is set. The matrix of required sensing values is denoted as $V(t) = \{V_{n,s}(t) | n \in \mathcal{N}, s \in \mathcal{S}\}$, where $V_{n,s}(t)$ denotes the required sensing value at cell n and timeslot s in the time period t . Based on actual sensing performance of drones according to Eq.(1), the sensing value collected by all drones observed by u at cell n and timeslot s is formulated as:

$$v_{n,s}(a^u, t) = p_{n,s}(a^u, t) \cdot V_{n,s}(t). \quad (2)$$

Matrix of target. In a real-world scenario, drones lack prior knowledge of the amount of required sensing values before they begin their sensing operations. Therefore, it becomes essential to build a target on the fly that instructs the drones regarding when and where they should or should not fly to given information from the environment. The matrix of the target is defined as $\mathcal{R}(t)$, which denotes the sensing requirements for all drones at period t . The element of the target is denoted as $r_{n,s}(t) = \{0, 1\}$, $n \in \mathcal{N}$, $s \in \mathcal{S}$, where $r_{n,s}(t) = 1$ requires only a drone to visit the cell n at timeslot s , and $r_{n,s}(t) = 0$ does not require sensor data collection by a drone.

Assumptions. To simplify the scenario, this paper makes the following assumptions: (i) Each drone is programmed to fly at a unique altitude while moving between cells to prevent collisions [32]. We also fix the ground speed of drones and the wind speed for simply calculating power consumption. (ii) Each time period concludes a flying period and a charging period: the time that drones perform sensing, and the time for charging. All drones finish charging before the next time period begins. We assume that each charging period is of equal duration and provides sufficient time for the drones to be fully charged. (iii) Each charging station is adequately equipped with charging capacity, enabling multiple drones to charge simultaneously without the need for queuing. This arrangement prevents any delays in the charging process.

B. Problem Formulation

We model the scenario of a swarm of drones that perform sensing by considering the following performance metrics: 1) mission efficiency; 2) sensing accuracy; and 3) energy cost.

Mission efficiency. It denotes the ratio of sensing values in all cells at all timeslots collected by the drones during their mission over the total required values in all cells at all timeslots during the period t . It is formulated as:

$$\text{Eff}(a^u, t) = \frac{\sum_{n=1}^N \sum_{s=1}^S v_{n,s}(a^u, t)}{\sum_{n=1}^N \sum_{s=1}^S V_{n,s}(t)}. \quad (3)$$

Sensing accuracy. It denotes the matching (correlation¹) between the total sensing values collected and the required ones. The metric is formulated as follows:

$$\text{Acc}(a^u, t) = \sqrt{\frac{N \cdot S}{\sum_{n=1}^N \sum_{s=1}^S [v_{n,s}(a^u, t) - V_{n,s}(t)]^2}}. \quad (4)$$

Energy cost. It is the energy consumed by drones to perform spatio-temporal sensing. A power consumption model [33] is used to calculate the power consumption with input the specification of drones (weight, propeller and power efficiency). This model estimates the cost of navigation and sensing plans, and emulates the outdoor environments [16]. The energy cost of each drone u is formulated as:

$$E(a^u, t) = C^f(u) \cdot t^f(a^u) + C^h(u) \cdot t^h(a^u), \quad (5)$$

where $C^f(u)$ and $C^h(u)$ are the flying and hovering power consumption of drone u respectively; t^f and t^h are the flying and hovering time respectively, which are determined by the sensing plan $P^u(a^u, t)$.

Overall performance. The optimization problem has three objectives: 1) maximize mission efficiency; 2) maximize sensing accuracy; and 3) minimize energy cost. Simultaneously achieving all of these objectives is a daunting task, as they often oppose each other. Maximizing both efficiency and accuracy is a trade-off since increasing efficiency of mission results in sensing imbalance and even blind areas by under-sensing [25]. In addition, in order to achieve both of these goals, drones have to continuously move to collect data from different cells, which results in higher energy costs due to long-distance flights. However, some trips of drones may not improve sensing quality in the long run. For instance, at the end of a period, drones opt to return to the nearest charging station where there are fewer sensing tasks in the next period. This choice reduces the energy cost of the current period but comes at the significant expense of sacrificing the sensing quality in the next period. Therefore, the overall sensing performance is optimized by integrating these opposing objectives and selecting the plans of each drone. The objective function is formulated as follows:

$$\arg \max_{a^u, u \in \mathcal{U}} \sum_{u=1}^U \sum_{t=1}^T [\text{Eff}(a^u, t) \cdot \text{Acc}(a^u, t) - E(a^u, t)]. \quad (6)$$

DRL Modeling. Once drones take actions of flying directions, they execute plans and return to charging stations, changing their current locations and battery levels while observing the navigation and sensing of other drones. Therefore, the problem scenario can be explained into a Markov decision process [26]. We model the problem using state, action, and reward concepts: (i) *State*: The state \mathbf{s}_t at period t consists of four components $(\mathcal{S}_1, \mathcal{S}_2, \mathcal{S}_3, \mathcal{S}_4)$, where $\mathcal{S}_1 = \{c^u(t) | u \in \mathcal{U}\}$ is the current locations of drones. Since drones charge at charging stations before taking actions, the location can serve as the index of the charging station. $\mathcal{S}_2 = \{e^u(t) | u \in \mathcal{U}\}$ is the current battery levels of drones, which are calculated based on

¹Error and correlation metrics (e.g. root mean squared error, cross-correlation or residuals of summed squares) estimate the matching, shown to be NP-hard combinatorial optimization problem in this context [8], [9].

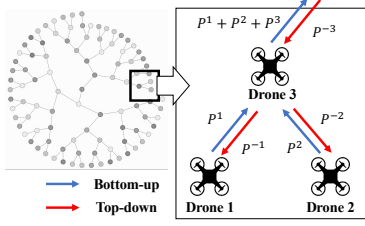


Fig. 1. Overview of the structured tree communication model. During the bottom-up process, Drone 3 aggregates the plans of its children, i.e., drone 1 and drone 2, and sends them to its parent agent with its own plan. During the top-down process, each parent agent sends the total aggregated plans to its children such that all agents obtain the observed plans.

the battery capacity and energy cost. $\mathcal{S}_3 = \{P^u(t)|_{u \in \mathcal{U}}\}$ is the plan of u . $\mathcal{S}_4 = \{P^{-u}(t)|_{u \in \mathcal{U}}\}$ is the aggregated plan of other drones excluding u , which are shared via the designed communication model. (ii) *Action*: The action $\mathbf{a}_t = \{a_t^1, \dots, a_t^U\}$ at period t consists of period-by-period flying directions (N, E, S, W, NE, SE, SW, NW or O) determined by drones. (iii) *Reward*: Based on the objective function of Eq.(6), the expected immediate local reward of one drone at period t is defined as follows: $\mathbf{r}_t^u = \text{Eff}(a^u, t) \cdot \text{Acc}(a^u, t) - E(a^u, t)$. Throughout the training process or episodes, the overall reward fluctuates based on the actions taken by the drones. This helps drones in prioritizing areas rich in sensor data by maximizing their reward, i.e., the highest cumulative overall performance.

C. Communication Model

In DRL model, each drone evaluates an immediate reward by considering collective information from other drones. To enhance information exchange efficiency, we design a structured tree communication model. Each drone, controlled by a local agent, connects with other agents into a tree communication structure, as shown in Fig. 1, within which it interacts with its children and parent in a bottom-up and top-down. For example, drones aggregate and share their plans P^u in a bottom-up fashion, and then obtain the observed plans P^{-u} in the top-down process [8]. Therefore, this decentralized coordination among agents is highly-efficient with low communication cost [8]. Through iterative bottom-up and top-down exchanges, agents can flexibly change their plans based on the aggregated navigation and sensing from other drones.

Furthermore, agents can be self-organized within the tree to make the system more resilient to attacks or failures [11], [12]. Since agents share the aggregated states instead of the agents' one, the system is scalable and designed to preserve privacy². For instance, assuming a swarm of drones that belong to various entities, such as aviation agencies, private citizens, and companies, they collaborate to create shared navigation and sensing strategies which rely on the collective sum of plans rather than individual private sensing information.

D. System Overview

For high-quality sensing performance, the proposed approach *DO-RL* relies on both decentralized drone coordination

²Additional privacy protection mechanisms such as differential privacy and homomorphic encryption apply here [34].

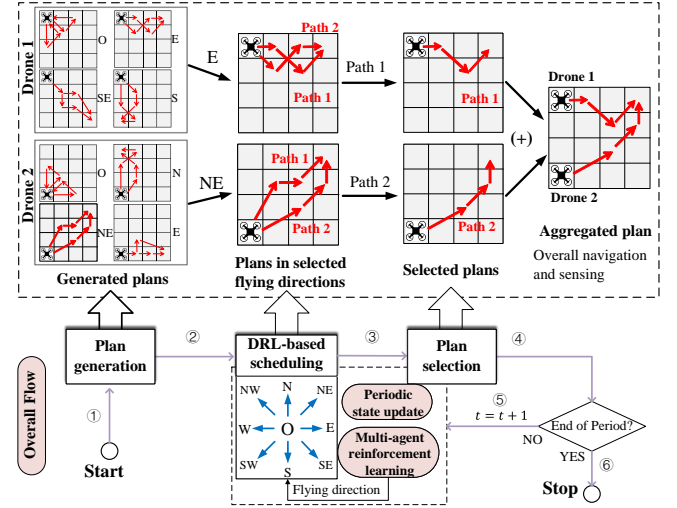


Fig. 2. System framework of *DO-RL*. The overall flow of *DO-RL* is depicted at the bottom; The plan selection is illustrated for two drones; The plan generation part outlines the procedure for generating a plan when drone 1 is traveling to the east.

for short-term navigation and sensing optimization, as well as long-term scheduling of flying directions to adapt to changing environments. Fig.2 illustrates the designed system framework of *DO-RL*, consisting of four main components:

Plan generation. This component generates the navigation and sensing options for drones. Given the sensing map, each drone autonomously generates a finite number of discrete plans to initialize the overall process. This provides flexibility for the drones at the next stage to choose in a coordinated way. The generated plans are grouped into different flying directions. This initialization stage is executed only once for each drone.

Plan selection. This distributed component leverages a collective learning to coordinate drones to locally select the optimal navigation and sensing options from their generated plans within a period.

DRL-based scheduling. This component is the core of the framework, which leverages the DRL algorithm to enable drones to take their period-by-period actions of flying directions. Then, the generated subset of plans with the corresponding navigation action are chosen as input for the plan selection. After plan selection, it undergoes two steps: one is periodic state update, which updates the state of drones (i.e., the current location and energy cost) and the system (i.e., the target and required sensing values) for the DRL-based scheduling in the next period; the other is multi-agent reinforcement learning, which is built based on centralized training and decentralized execution.

IV. DETAILED SYSTEM DESIGN

A. Plan Generation

Each drone generates nine groups of plans, each associated with an action for a flying direction. These groups consist of multiple individual plans of the same size. A group of plans generated by drone u during a period is defined as

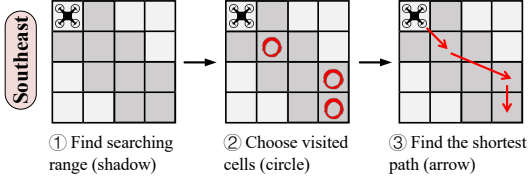


Fig. 3. Process of path finding in plan generation.

$G^a(t)$, where each plan in the group has the same action, $P^u(a^u, t) \in G^a(t)$. Then, a plan can be defined as $P^u(a^u, t) = \{l, K(a^u), J(a^u), E(a^u, t)\}$, where l is the index of the plan, $l \leq L$, (L denotes the total number of plans in a group); $K(a^u)$ denotes the indexes of cells within the searching range along flying direction a^u ; $J(a^u)$ denotes the indexes of visited cells within $K(a^u)$; and $E(a^u, t)$ denotes the energy consumed by u traveling over $J(a^u)$, i.e., the cost of the plan.

A drone generates a plan by determining its path and calculating the energy required for traversing that path, as shown in Fig. 3. As an example of a plan, the drone u firstly finds a searching range to cells $K(a^u)$: it determines a range with a certain width (equal to half of distance to nearest charging station) along its flying direction, and then searches the cells within this range. Next, it selects the visited cells $J(a^u)$ randomly from this range. Then, u finds the shortest possible path among $J(a^u)$ via the *Dijkstra's algorithm* for the Traveling Salesmen Problem. The path includes the information of which cell and which timeslot the drone uses to collect data, and thus both the traveling time $t^f(a^u)$ and hovering time $t^h(a^u)$ are calculated. The total energy consumption $E(a^u, t)$ when u travels over the path is then calculated via Eq.(5).

B. Plan Selection

Given the plans in selected flying directions within a period, drones can adapt their assignments by selecting appropriate plans in response to changes in task targets, enhancing their flexibility and adaptability in dynamic environments. In this process, the agents of drones improve their plan selections based on the structured tree communication model. Specifically, each agent obtains the aggregated choices, i.e., the aggregated plan $P^{-u}(a^u, t)$, from other agents, and chooses one of the plans $P^u(a^u, t, l)$ such that all choices together $P^u(a^u, t) + P^{-u}(a^u, t)$ add up to match a target $\mathcal{R}(t)$. The target is used to steer each drone to sense over a unique cell during a timeslot, thereby avoiding the simultaneous sensing of multiple drones within the same cell, i.e., preventing over-sensing and under-sensing.

The purpose of coordination is to match the aggregated plans of all agents to the target while minimizing the energy cost $E(a^u, t)$ of the plan selected by the drone. The cost function for each agent is formulated using the root mean square error (RMSE):

$$\min_{a^u, u \in \mathcal{U}} (1 - \beta) \cdot \sqrt{\frac{\sum_{n=1}^N \sum_{s=1}^S [p_{n,s}(a^u, t) - r_{n,s}(t)]^2}{N \cdot S}} + \beta \cdot E(a^u, t), \quad (7)$$

where β represents the behavior of an agent. As the value of β increases, the agent becomes increasingly selfish, prioritizing plans with lower energy costs at the expense of higher root mean squared error. Each agent (or drone) aims to minimize the system-wide cost of sensing while considering its energy consumption. By minimizing this cost function, each drone coordinates to select its optimal plan, indicating a specific path within a period (comprising multiple timeslots). Via planning and selection, drones using *DO-RL* only need to take high-level actions of flying directions in each period, and thus reducing the number of decisions and observations in DRL.

C. Periodic State Update

After choosing a plan, each drone changes its current state at the next period $t + 1$, including its location $c^u(t + 1)$, battery level $e^u(t + 1)$, selected plan $P^u(t + 1) := P^u(a^u, t)$, and observed plans $P^{-u}(t + 1) := P^{-u}(a^u, t)$. However, due to dynamic changing environment, drones have no knowledge about the required sensing value in the next period. They need to predict and estimate the required sensing value to calculate reward function via Eq.(3) and (4). Depending on the predicted distribution of sensor data, the target is required to be updated.

Predicted sensing value. The predicted sensing value at period t , denoted as $\hat{V}(t)$, is updated in a time-reverse decay, formulated as follows:

$$\hat{V}_{n,s}(t) = \sum_{t'=1}^t (T - t + t') \cdot \omega_{n,s}(t') \cdot v'_{n,s}(a^u, t') := V_{n,s}(t), \quad (8)$$

where $V'_{n,s}$ denotes the data values collected by drones once they execute their selected plans (the total collected values are aggregated and shared to each agent via the top-down interactions in the distributed optimization process [8]); $\omega_{n,s}(t')$ is a prediction coefficient such that $0 < \omega_{n,s}(t') < 1$, $t' \leq t$. To achieve accurate predictions, *DO-RL* leverages the Ordinary Least Squares regression method (OLS) to train these coefficients initially, and use the past experienced observations as the target distribution for training. After that, the current collected data values $V'_{n,s}$ and predicted one $\hat{V}_{n,s}$ are shared to all agents via the tree communication structure.

Target. The target \mathcal{R} in the plan selection needs to be iteratively updated to steer the coordination of drones to choose plans for areas and timeslots with abundant sensor data. The percentile-based data filtering is used to eliminate the extreme low sensing values collected by drones. This approach effectively removes the need for data collection in regions with low sensing requirements (e.g., traffic exclusion zones). As a consequence, it helps drones in prioritizing their operations in cells and time where sensing values are significantly high. We initialize the target as $r_{n,s}(0) = 1$ to encompass all cells and timeslots, and update it as follows:

$$r_{n,s}(t) = \begin{cases} 0, & v'_{n,s}(a^u, t) < \bar{v} \wedge p_{n,s}(a^u, t) > 0 \\ r_{n,s}(t - 1), & \text{otherwise} \end{cases}, \quad (9)$$

where the threshold \bar{v} is set iteratively and calculated as the value at the $100(1 - U/N)$ th percentile among the predicted data values $\hat{V}_{n,s}(t)$.

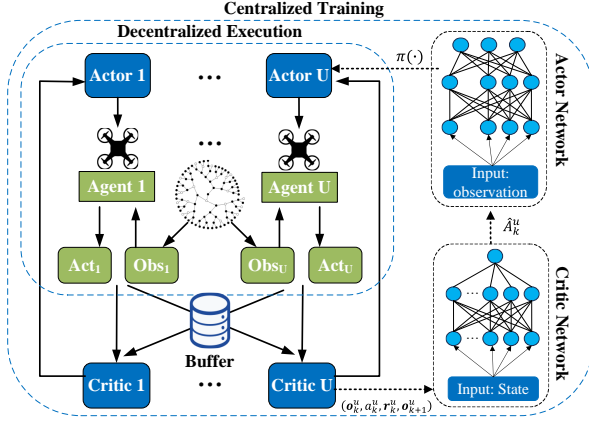


Fig. 4. DRL-based long-term scheduling overview.

D. Multi-agent Reinforcement Learning

Our approach provides a generalized model for multi-agent reinforcement learning by adopting the framework of centralized training and decentralized execution, as shown in Fig. 4. During execution, each agent obtains a local aggregated observation comprising both private and public information. Apart from their own private data such as locations, battery levels, and selected plans, this observation contains aggregated plans shared via the designed communication model (shown in Fig. 1). The training part is built based on an actor-critic model. The actors allow drones to work independently and choose actions based on their observations and policies, allowing for parallel data collection and processing. The critic, however, evaluates the actions of drones and guide them toward collectively optimal decisions. In addition, *DO-RL* employs Proximal Policy Optimization (PPO) to prevent detrimental updates and improving the stability of the learning process [35].

The process of training primarily involves the following steps: Firstly, each agent takes an action for a flying direction based on the aggregated observation \mathbf{o}_t^u shared via coordination as well as the reward \mathbf{r}_t^u . Once all actions are determined, drones select their plans and transition to a new state. Subsequently, the buffer, a data storage structure used for experience replay, stores all transitions of each agent $(\mathbf{o}_t^u, \mathbf{a}_t^u, \mathbf{r}_t^u, \mathbf{o}_{t+1}^u)$. Several groups of transitions $(\mathbf{o}_k^u, \mathbf{a}_k^u, \mathbf{r}_k^u, \mathbf{o}_{k+1}^u)$ are sampled randomly (H groups of transitions) for updating the parameters of both the critic and actor networks. The algorithm is typically an extension of the actor-critic policy gradient approach, employing two deep neural networks for each agent: a critic network $Q(\cdot)$ and an actor network $\pi(\cdot)$. The critic network estimates the reward associated with a transition using Bellman equation, and its parameter θ^Q is then updated by minimizing a loss function $L(\theta^Q)$:

$$L(\theta^Q) = \frac{1}{H \cdot U} \sum_{k=1}^H \sum_{u=1}^U (\hat{A}_k^u)^2, \quad (10)$$

$$\hat{A}_k^u = \mathbf{r}_k^u + \gamma \cdot Q(\mathbf{o}_{k+1}^u, \mathbf{a}_{k+1}^u) - Q(\mathbf{o}_k^u, \mathbf{a}_k^u), \quad (11)$$

where γ is a discount factor; \hat{A}_k^u is an advantage function. Then, the critic network provides \hat{A}_k^u to the actor network to

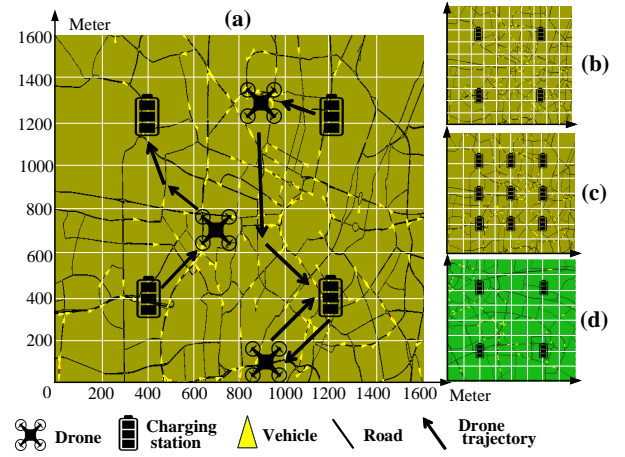


Fig. 5. The central business district of Munich, Germany: (a) Basic scenario with 64 cells, 4 charging stations and high density of vehicles; (b) Increase the number of cells to 100; (c) Increase the number of charging stations to 9; (d) Change to a new map with low density of vehicles.

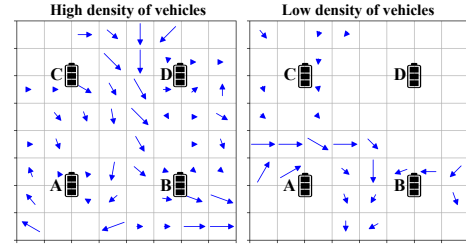


Fig. 6. The distribution of both charging stations and traffic vehicles in the maps with high and low density of vehicles. There are 4 charging stations uniformly distributed in the map with $64 = 8 \times 8$ cells lined up over the map. The blue arrows symbolize the flow of vehicular traffic, with their length proportional to the volume of vehicles over 8 periods.

increase the probability of actions that have a positive impact and decrease the ones that have negative impact. The actions are taken by drones as $\mathbf{a}_t^u = \pi(\mathbf{o}_t^u)$. The parameter θ^π of the actor network is updated by maximizing the clip objective $L_{CLIP}(\theta^\pi)$, as follows [35]:

$$L_{CLIP}(\theta^\pi) = \frac{1}{H \cdot U} \sum_{k=1}^H \sum_{u=1}^U \min(\text{ratio}(\theta^\pi, u) \hat{A}_k^u, \text{clip}(\text{ratio}(\theta^\pi, u), 1 - \epsilon, 1 + \epsilon) \hat{A}_k^u), \quad (12)$$

where ϵ is a hyperparameter; $\text{clip}(\cdot)$ defines the surrogate objective by limiting the range of $\text{ratio}(\theta^\pi, u) = \frac{\pi(\mathbf{a}_k^u | \mathbf{o}_k^u)}{\pi_{old}(\mathbf{a}_k^u | \mathbf{o}_k^u)}$ using clipping, thereby eliminating incentives to exceed the interval $[1 - \epsilon, 1 + \epsilon]$; π_{old} denotes the older policy of the actor network in the previous iteration.

V. PERFORMANCE EVALUATION

In this section, an overview of the experimental settings is presented. The sensor dataset, specification of drones, optimization algorithm employed, and the used neural network are introduced. Then, the baselines and performance evaluation metrics are discussed. Finally, the results are assessed across various scenarios.

A. Experimental Settings

Scenario model. In order to evaluate the *DO-RL*, we model a real-world transportation scenario, where a swarm of drones perform the sensing tasks of traffic monitoring. The number of vehicles serves as the required sensing value in the model. Drones rely on accurate vehicle observation to detect early signs of traffic congestion. This enables traffic operators to apply mitigation measures, reducing the carbon footprint in one of the world's highest-emission sectors.. The scenario involves a real-world map of Munich city, imported to the simulations of urban mobility (SUMO)³ to accurately generate realistic flows of vehicles. Fig. 5 illustrates a selected map of 1600×1600 meters in the city with the simulation time of 50 hours, which is 100 periods. It has a high density of vehicles, approximately 2,000 vehicles passing by per hour. The area split into a finite number of cells, each is defined as a rectangular square with the size of 200×200 meters that can be captured by the cameras of drones. Fig. 6 shows the distribution of both charging stations and traffic vehicles in the map. The charging stations are uniformly distributed in the map. We employ cross-validation: 80% simulation time of the datasets for training and 20% for testing. There are two scenarios for the experimental evaluation in this paper: (i) *Basic scenario*. It has 64 cells, 4 charging stations and 8 time periods (set as 30min for each period). It has high density of vehicles, around 2,000 vehicles passing by per time period. 16 drones sense the area (camera recording) in parallel. (ii) *Complex scenario*. It varies the parameter settings such as the density of drones and vehicles, as well as the number of time periods, cells and charging stations.

Drones. We assume that all drones are of the same type, specifically the DJI Phantom 4 Pro model⁴. Each drone has a body weight of 1.07 kg and four propellers, each with a diameter of 0.35 m. The ground speed of the drones is set at 6.94 m/s, and the drag force is determined to be 4.1134 N [33]. As a consequence, the power consumption remains consistent across all drones. Additionally, drones are equipped with a 6000 mAh LiPo 2S battery (0.31 kg) [36]. The maximum flying time for drones is approximately 30 min, which is set as one flying period. A flying period has $S = 30$ timeslots, each of one minute. Moreover, to ensure that the camera covers the entire area of a cell (see Fig. 5), the minimum hovering height of drones is determined at which the field of view of the camera and the cell overlap. The hovering height h is calculated based on the distance between any two cells (approximately 200 meters), the camera resolution, focal length derived from camera calibration, and ground sampling distance [37]. Therefore, each drone equipped with a 4K camera senses from a minimum height of 82.4 meters.

Planning and distributed optimization. We leverage the decentralized multi-agent collective learning method of *EPOS*⁵, the *Economic Planning and Optimized Selections* [8]. We generate $L = 64$ plans for each agent. All generated plans

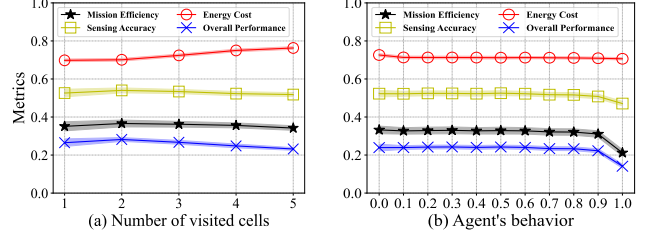


Fig. 7. *DO-RL* has its peak overall performance when $J_u = 2$, $\beta \in [0.1, 0.8]$. Change the parameters of *DO-RL* in mobility range and agents' behavior.

are made openly available to encourage further research on coordinated spatio-temporal sensing of drones [13], [16], [25]. Each agent in *EPOS* is mapped to a drone. During the coordinated plan selection via *EPOS*, agents self-organize into a balanced binary tree as a way of structuring efficient learning interactions [38]. The shared goal of the agents is to minimize the RMSE between the total sensing values collected and the target via Eq.(7). In the one execution of *EPOS*, the agents perform 40 bottom-up and top-down learning iterations during which RMSE converges to a minimum optimized value. To minimize the RMSE and the cost of plans, we make an empirical choice of parameters, such as the number of visited cells (mobility range) $J^u = 2$ and the behavior of agents β within a range $[0.1, 0.8]$. The results are shown in Fig. 7.

Neural network and learning algorithm. We sample $H = 64$ groups of transitions as minibatches in a replay buffer, and set the discount factor as $\gamma = 0.95$ and the clip interval hyperparameter to 0.2 for policy updating. Then we try different multi-layer perceptions (MLP), and use $W = 64$ neurons in the three hidden layers of the MLP in both critic and actor networks. The activation function used for the networks is tanh. We train the models for $\mathcal{E} = 5000$ episodes with multiple epochs (i.e., time period).

Complexity. Given the number of nodes per layer W , number of episodes \mathcal{E} , size of state space \mathcal{X} , and number of actions A , the computational complexity of DNN is approximately $O(C_{dnn}) := O((\mathcal{X} + A)W + 3W^2)$ [18]. The comparison of both computational and communication cost is shown in Table III, where I denotes the number of iterations in *EPOS*.

TABLE III
COMPARISON OF COMPUTATIONAL AND COMMUNICATION COSTS.

Attributes	Approaches:	<i>EPOS</i> [8]	<i>MAPPO</i> [17]	<i>DO-RL</i>
Computational Cost		$O(LI \log U)$	$O(ETSC_{dnn})$	$O(ET(C_{dnn} + LI \log U))$
Communication Cost		$O(I \log U)$	$O(U^2)$	$O(I \log U)$

B. Baselines and Metrics

We compare *DO-RL* with the following baseline methods:

Greedy. It aims to assign each drone to a single cell, enabling it to accomplish the necessary sensing tasks within a time period [21]. This algorithm minimizes the number of visited cells and travel distance, resulting in reduced energy consumption for drones. To promote decentralization, we

³<https://www.eclipse.org/sumo/>

⁴<https://www.dji.com/uk/phantom-4-pro/info>

⁵*EPOS* is open-source and available at: <https://github.com/epourmaras/EPOS>.

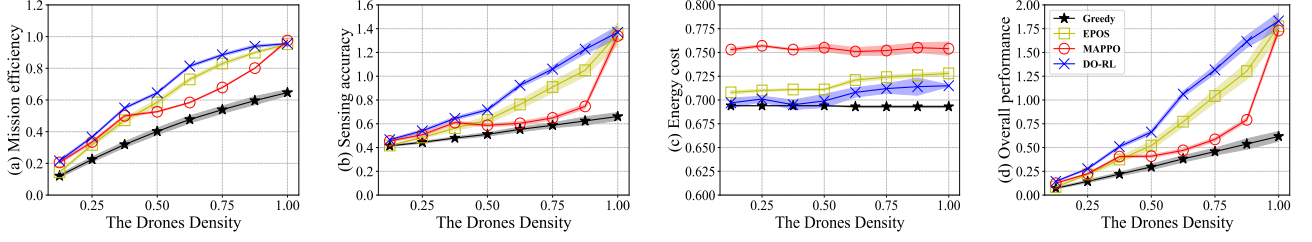


Fig. 8. **High density of drones increases both mission efficiency and sensing accuracy of all methods, especially for short-term optimization methods (*DO-RL* and *EPOS*).** *DO-RL* also shows its superior performance across different drones densities. Changing the drones density by increasing the number of drones from 8 to 64 and fixing 8 periods, 64 cells, 4 charging stations and high density of vehicles.

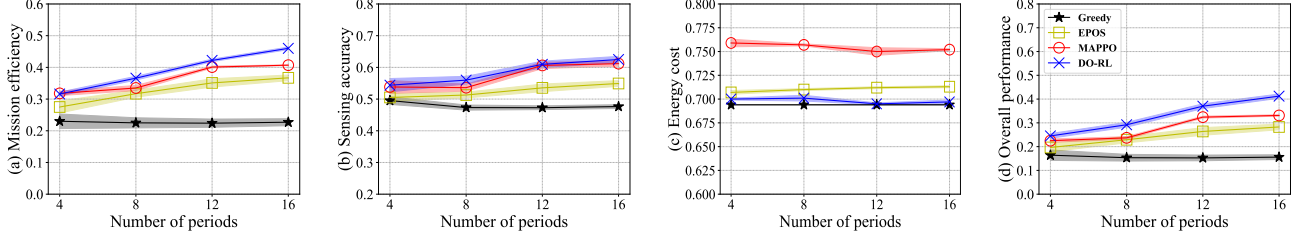


Fig. 9. **High number of periods increases both mission efficiency and sensing accuracy of all methods, especially for long-term learning methods (*DO-RL* and *MAPPO*).** *DO-RL* also shows its superior performance across different number of periods. Changing the the number of periods from 4 to 16 and fixing 16 drones, 64 cells, 4 charging stations and high density of vehicles.

implement the algorithm with a local view for each drone, i.e., they have no coordination or awareness of cell occupancy by other drones. By adopting this approach, we ensure an energy-efficient and independent operation of each drone.

EPOS. It is designed to select the optimal plan for drones based on the generated plans [8]. It incorporates the plan generation and the periodic state update, but does not support any long-term strategic navigation. Agents randomly choose any charging station to land on at every period.

MAPPO. It is one state-of-the-art DRL algorithm using PPO [35], but does not include distributed optimization compared to *DO-RL*. Moreover, agents in *MAPPO* learn the flying directions timeslot by timeslot, rather than period by period as in *DO-RL*. At each timeslot, a drone takes actions to horizontally move to an adjacent cell in eight directions or hover (similar to the actions in *DO-RL*), and returns to the nearest charging station at the end of every S timeslots (one period). For fair comparison, this method employs the same reward function and structured tree communication model to share the aggregated observation.

The evaluation of all algorithms includes three key metrics: 1) *Mission efficiency*, 2) *Sensing accuracy* and 3) *Energy cost*. These metrics are determined using Eq.(3), (4) and (5) respectively. We use the number of vehicles detected/observed by drones to represent the sensing values defined in this paper. Furthermore, to obtain a comprehensive assessment that considers all three metrics, we conduct an overall performance evaluation using Eq.(6).

C. Results and Analysis

There are six dimensions for the complex scenario we study here: (i) the density of drones, (ii) the number of periods, (iii)

the number of cells, (iv) the number of charging stations, (v) the density of vehicles, (vi) the number of drones and cells while fixing the density of drones, (vii) the remaining battery level, and (viii) the charging load. Results are shown in Fig. 8-13, where the shadow area around the lines represents the standard deviation error of the results.

Density of drones. It denotes the ratio of the number of drones over the number of cells, representing the coverage of a single drone in the map. In this case, we fix the number cells as 64, and increase the number of drones from 8 to 64, that is, the drones density increases from 0.125 to 1.0. Fig. 8 illustrates the performance of *DO-RL* and the three baseline methods when using different drones density to perform traffic monitoring. As drones density increases, both mission efficiency and sensing accuracy of *DO-RL* increase linearly. These are approximately 23.0% and 15.8% higher than *EPOS* respectively, as shown in Fig. 8(a) and Fig. 8(b)⁶. This is because *DO-RL* controls the traveling direction of drones based on the predicted sensor data, so that drones cover the area with the maximum sensing value. *MAPPO* has high efficiency and accuracy with a low density of drones (maximum p-value less than 0.001 using Mann-Whitney U test), but its performance degrades when the drones density is higher than 0.375 due to the high computational complexity. In contrast, the plan selection in *DO-RL* reduces the action space and mitigates the learning difficulty, resulting in high performance with a high number of drones. In Fig. 8(c), the energy cost of *DO-RL* is on average 1.7% lower than

⁶*DO-RL*, *EPOS* and *MAPPO* have similar overall performance when the density of drones is 1.0, with maximum p-value of 0.04, because there are ample drone resources available to effectively coordinate the coverage of the entire area.

	Mission Efficiency				Sensing Mismatch				Energy Cost				Overall Performance																				
	Greedy	EPOS	MAPPO	DO-RL	Greedy	EPOS	MAPPO	DO-RL	Greedy	EPOS	MAPPO	DO-RL	Greedy	EPOS	MAPPO	DO-RL																	
cells=64 stations=4	0.23	0.23	0.32	0.32	0.34	0.51	0.34	0.53	0.47	0.48	0.51	0.51	0.54	0.82	0.61	0.93	0.69	0.69	0.71	0.71	0.75	0.77	0.71	0.71	0.16	0.17	0.23	0.23	0.24	0.55	0.29	0.69	
cells=100 stations=4	0.15	0.15	0.17	0.20	0.19	0.36	0.27	0.40	0.53	0.53	0.53	0.54	0.56	0.86	0.60	0.88	0.69	0.69	0.71	0.71	0.75	0.75	0.70	0.70	0.12	0.12	0.13	0.15	0.14	0.42	0.23	0.49	
cells=64 stations=9	0.23	0.23	0.29	0.29	0.40	0.50	0.31	0.57	0.47	0.47	0.49	0.49	0.59	0.84	0.52	0.89	0.69	0.69	0.71	0.71	0.74	0.75	0.70	0.70	0.16	0.16	0.20	0.20	0.32	0.56	0.23	0.72	
cells=100 stations=9	0.15	0.15	0.20	0.21	0.19	0.31	0.28	0.47	0.53	0.52	0.54	0.55	0.56	0.83	0.60	0.98	0.69	0.69	0.70	0.71	0.75	0.75	0.70	0.70	0.12	0.12	0.15	0.17	0.14	0.34	0.24	0.66	
	High	Low	High	Low	High	Low	High	Low	High	Low	High	Low	High	Low	High	Low	High	Low	High	Low	High	Low	High	Low	High	Low	High	Low	High	Low	High	Low	

Fig. 10. Both low number of cells and high number of charging stations increase the overall performance of all methods. Long-term learning methods outperform short-term optimization methods in observing traffic flow when vehicles are sparsely distributed across the map. Performance comparison under varying parameters: the number of cells (64 and 100), the number of charging stations (4 and 9), and the density of vehicles (high and low). The red palette on the right represents the values of energy cost, while the blue one denotes the values of mission efficiency, sensing mismatch and overall performance.

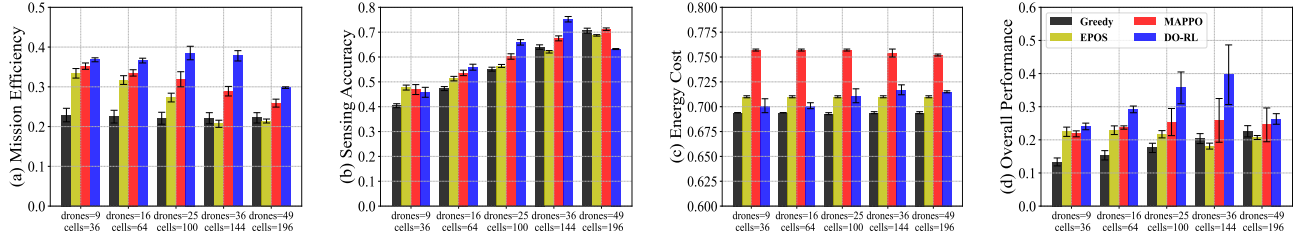


Fig. 11. High number of drones/cells with fixed drones density increases the sensing accuracy of all methods, peaking at 36 drones and 144 cells. Changing the number of drones and cells but fixing the drones density at 0.25 with 8 periods, 4 charging stations and high density of vehicles.

EPOS and 7.9% lower than *MAPPO*. *Greedy* has the minimum energy cost among all methods, only 7.89% lower than *DO-RL*, but has the lowest performance in efficiency and accuracy.

Number of periods. As shown in Fig. 9, *DO-RL* achieves superior performance compared to other methods, increasing linearly as the number of periods increase (increased by 51.3% in quadruple time). Although it has statistically similar mission efficiency to *MAPPO* when the number of periods is 4, this metric increases dramatically because drones update and obtain more accurate predicted sensor data with higher number of periods. The timeslot-by-timeslot learning in *MAPPO* perplexes the actions learned by drones compared to *DO-RL*, since drones only take actions once per period (30min) in *DO-RL* but take actions per minute in *MAPPO*. This also results in higher flying energy consumed by drones, and thus the energy cost of *MAPPO* is around 8.1% higher than *DO-RL*.

Fig. 10 illustrates the performance comparison between *DO-RL* and the three baseline methods, varying the number of cells, charging stations and the density of vehicles, while keeping the number of drones fixed at 16 and the number of periods at 8.

Number of cells. If the number of cells increases from 64 to 100, the density of drones decreases. In Fig. 10, *DO-RL* shows a lower decrease in mission efficiency (decreased by 27.04%) than *MAPPO* (decreased by 44.50%) and *EPOS* (decreased by 45.11%) as the number of cells increases. Furthermore, *DO-RL* keeps relatively constant both sensing accuracy and energy cost as the number of cells varies.

Number of charging stations. If the number of charging

stations increases from 4 to 9, the distance between the sensing areas and stations is reduced, cutting down the energy cost of recharging. As a result, the overall performance of both *DO-RL* and *EPOS* increase by 19.52% and 14.35% respectively.

Density of vehicles. If we select a new map area that has low density of vehicles, the distribution of sensor data changes (with different road distribution), as shown in Fig. 6. In Fig. 10, both *DO-RL* and *MAPPO* have higher mission efficiency and sensing accuracy than the other two methods, with an average of 90.65% higher efficiency and 76.85% higher accuracy. This is because the learning methods observe the environment and control drones to collect data in the cells and timeslots with the highest number of vehicles. *DO-RL* performs better than other methods under low density of vehicles even though the number of cells and charging stations increase.

Number of drones/cells with fixed drones density. If we fix the density of drones but increase the number of drones, the number of cells increases proportionally. For example, we use the density of drones in the basic scenario of 0.25, and increase the number of drones from 9 to 49 and the number of cells from 36 to 196. As shown in Fig. 11, when the number of drones/cells increases, the sensing accuracy of all methods increases. However, the mission efficiency of both *EPOS* and *MAPPO* decreases (by 35.93% and 26.42% respectively). This is due to *EPOS* facing challenges in efficiently scheduling drones for a large number of cells, while *MAPPO* experiences increased computational complexity. In contrast, *DO-RL* overcomes these challenges and demonstrates a 4.62% increase in mission efficiency. When increasing to

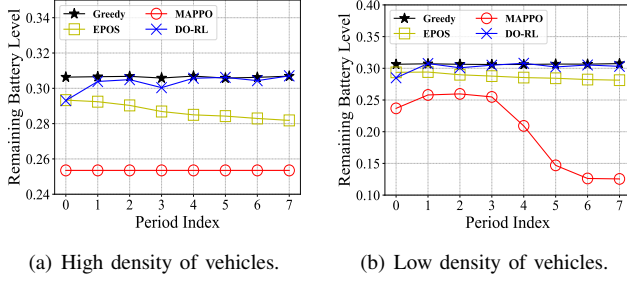


Fig. 12. **DO-RL keeps drones at a safe remaining battery level before recharging.** Performance comparison of the remaining battery level of four methods on both high and low density of vehicles.

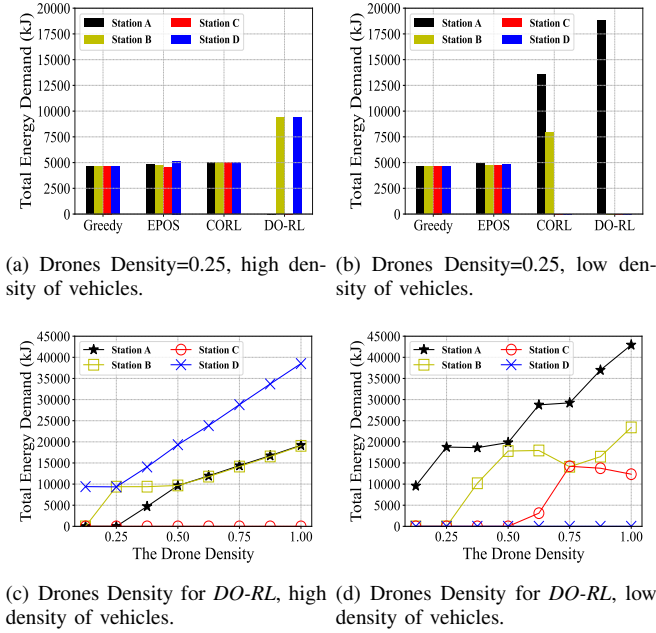


Fig. 13. **DO-RL relies on a lower number of charging places compared to other methods.** Performance comparisons of the total energy demand of four methods with 0.25 density of drones, see (a) and (b), and the DO-RL with different density of drones, see (c) and (d). Both comparisons are categorized by the high and low density of vehicles, see Fig. 6.

49 drones and 196 cells, however, the sensing accuracy of *DO-RL* degrades, decreased by 15.96%, due to the high complexity of scheduling and computation. In overall, *DO-RL* has statistically higher overall performance than other methods, with an average improvement of 46.98% (maximum p-value less than 0.001), which confirms the efficiency of the proposed method.

Remaining battery level. It denotes a percentage of battery level once drones have completed their sensing tasks. The value is calculated as an average among all drones within each time period. As shown in the Fig. 12(a) and 12(b), *DO-RL* keeps drones at a high remaining battery level on high and low density of vehicles, with approximately 30.25% and only 1.05% lower than *Greedy*. This level follows the drones' safety regulations which suggest finishing the missions when battery life is around 25% – 30%. However, *MAPPO* does not meet the regulations under low density of vehicles, and the

minimum battery level can reach 12.55%.

Charging load. It is the total energy demand of drones on each charging station over all time periods. This aims to study the placement of charging stations. As shown in the Fig. 13(a) and 13(b), the total energy demand on charging stations of *DO-RL* over all periods is more imbalanced compared to other methods. This is because with *DO-RL* drones learn to travel to the areas with the high required sensing data values. Since drones set the nearest charging stations as destinations, they rely on a lower number of charging places. For example, as shown in Fig. 13(c) and 13(d), when the density of drones is 0.125 under high density of vehicles, drones only depart from and return to the charging station *D* since the vehicle distribution around *D* is more dense than other charging stations. As the density of drones becomes 1, drones gradually rely on the charging station *B* and *D*. Similarly, drones only need to fly over the vehicle-dense areas around the charging station *A* and *B* under low density of vehicles. These results provide insights to policy makers for providing higher amount of energy on vehicle-dense areas to support the charging of drones.

In summary, **several scientific insights** on experimental results are listed as follows: (i) Under scarce drone resources, it is more efficient and accurate to employ long-term learning methods for optimizing sensing. In contrast, under abundant drone resources, short-term optimization methods alone suffice. (ii) Long-term learning methods optimize drone resource usage for traffic management by directing drones towards regions with high vehicle density and advising on infrastructure planning for charging. (iii) With the help of short-term optimization, long-term learning can effectively prevent energy wastage, ensuring that drones maintain their battery levels above safety thresholds.

VI. CONCLUSION AND FUTURE WORK

This paper introduces a new approach named *DO-RL* to solve the navigation, sensing and recharging problem by a swarm of drones in a distributed and cost-effective manner. *DO-RL* leverages the DRL to determine the flying directions of drones period by period, and coordinates energy-aware drones to autonomously plan their navigation and sensing within each period using distributed optimization. Extensive experimentation using simulations of realistic urban mobility reveals the effectiveness of *DO-RL*: Drones can monitor traffic flow and provide valuable data for optimizing transportation systems and urban planning, ultimately contributing to more efficient and sustainable cybernetic cities. Furthermore, the proposed method effectively optimizes resource utilization, including drone resources, battery safety, and charging. This efficient allocation enables cybernetic systems to scale their drone fleets without significantly increasing resource demands.

However, the designed framework can be further improved towards several research avenues: 1) Use of simulated and real-world datasets in other applications of Smart Cities, including disaster response and smart farming. 2) Research of the real-time decentralized drone testbed to validate the applicability and realism of the proposed method.

ACKNOWLEDGEMENTS

This research is supported by a UKRI Future Leaders Fellowship (MR/W009560/1): *Digitally Assisted Collective Governance of Smart City Commons—ARTIO*, and the European Union, under the Grant Agreement GA101081953 for the project H2OforAll—*Innovative Integrated Tools and Technologies to Protect and Treat Drinking Water from Disinfection Byproducts (DBPs)*. Views and opinions expressed are, however, those of the author(s) only and do not necessarily reflect those of the European Union. Neither the European Union nor the granting authority can be held responsible for them. Funding for the work carried out by UK beneficiaries has been provided by UKRI under the UK government's Horizon Europe funding guarantee [grant number 10043071]. Thanks to Manos Chaniotakis and Zeinab Nezami for the support on the transportation datasets.

REFERENCES

- [1] Tejasvi Alladi, Vinay Chamola, Nishad Sahu, and Mohsen Guizani. Applications of blockchain in unmanned aerial vehicles: A review. *Vehicular Communications*, 23:100249, 2020.
- [2] Emmanouil Barmounakis and Nikolas Geroliminis. On the new era of urban traffic monitoring with massive drone data: The pneumonia large-scale field experiment. *Transportation research part C: emerging technologies*, 111:50–71, 2020.
- [3] Min Deng, Baoju Liu, Sumin Li, Ronghua Du, Guohua Wu, Haifeng Li, and Ling Wang. A two-phase coordinated planning approach for heterogeneous earth-observation resources to monitor area targets. *IEEE Transactions on Systems, Man, and Cybernetics: Systems*, 51(10):6388–6403, 2020.
- [4] Prithvi Krishna Chittoor, Bharatiraja Chokkalingam, and Lucian Mihet-Popa. A review on UAV wireless charging: Fundamentals, applications, charging techniques and standards. *IEEE Access*, 9:69235–69266, 2021.
- [5] Sabitri Poudel and Sangman Moh. Task assignment algorithms for unmanned aerial vehicle networks: A comprehensive survey. *Vehicular Communications*, page 100469, 2022.
- [6] Jingjing Cui, Yuanwei Liu, and Arumugam Nallanathan. Multi-agent reinforcement learning-based resource allocation for UAV networks. *IEEE Transactions on Wireless Communications*, 19(2):729–743, 2019.
- [7] Ryan Lowe, Yi I Wu, Aviv Tamar, Jean Harb, OpenAI Pieter Abbeel, and Igor Mordatch. Multi-agent actor-critic for mixed cooperative-competitive environments. *Advances in neural information processing systems*, 30, 2017.
- [8] Evangelos Pournaras, Peter Pilgerstorfer, and Thomas Asikis. Decentralized collective learning for self-managed sharing economies. *ACM Transactions on Autonomous and Adaptive Systems*, 13(2):1–33, 2018.
- [9] Evangelos Pournaras. Collective learning: A 10-year odyssey to human-centered distributed intelligence. In *2020 IEEE International Conference on Autonomic Computing and Self-Organizing Systems (ACSOS)*, pages 205–214. IEEE, 2020.
- [10] Sriyani Majumdar, Chuhao Qin, and Evangelos Pournaras. Discrete-choice multi-agent optimization: Decentralized hard constraint satisfaction for smart cities. *International Conference on Autonomous Agents and Multiagent Systems*. Springer, 2023.
- [11] Evangelos Pournaras, Srivatsan Yadhunathan, and Ada Diaconescu. Holarchic structures for decentralized deep learning: a performance analysis. *Cluster Computing*, 23(1):219–240, 2020.
- [12] Jovan Nikolic and Evangelos Pournaras. Structural self-adaptation for decentralized pervasive intelligence. In *22nd Euromicro Conference on Digital System Design (DSD)*, pages 562–571. IEEE, 2019.
- [13] Chuhao Qin and Evangelos Pournaras. EPOS-based Plans for Iterative Sensing and Charging. 11 2023. doi = "https://doi.org/10.6084/m9.figshare.24476533.v2".
- [14] Mehdi Alighanbari and Jonathan How. Robust decentralized task assignment for cooperative UAVs. In *AIAA Guidance, Navigation, and Control Conference and Exhibit*, page 6454, 2006.
- [15] Jie Chen, Xianguo Qing, Fang Ye, Kai Xiao, Kai You, and Qian Sun. Consensus-based bundle algorithm with local replanning for heterogeneous multi-UAV system in the time-sensitive and dynamic environment. *The Journal of Supercomputing*, 78(2):1712–1740, 2022.
- [16] C Qin, F Candan, L Mihaylova, and E Pournaras. 3, 2, 1, drones go! A testbed to take off UAV swarm intelligence for distributed sensing. In *Proceedings of the 2022 UK Workshop on Computational Intelligence*. Springer Nature, 2022.
- [17] Lige Ding, Dong Zhao, Mingzhe Cao, and Huadong Ma. When crowdsourcing meets unmanned vehicles: Toward cost-effective collaborative urban sensing via deep reinforcement learning. *IEEE Internet of Things Journal*, 8(15):12150–12162, 2021.
- [18] Babatunji Omoniwa, Boris Galkin, and Ivana Dusparic. Communication-enabled deep reinforcement learning to optimise energy-efficiency in UAV-assisted networks. *Vehicular Communications*, 43:100640, 2023.
- [19] Dong Zhao, Mingzhe Cao, Lige Ding, Qiaoyue Han, Yunhao Xing, and Huadong Ma. Dronesense: Leveraging drones for sustainable urban-scale sensing of open parking spaces. In *IEEE INFOCOM - Conference on Computer Communications*, pages 1769–1778. IEEE, 2022.
- [20] Moataz Samir, Chadi Assi, Sanaa Sharafeddine, Dariush Ebrahimi, and Ali Ghayeb. Age of information aware trajectory planning of UAVs in intelligent transportation systems: A deep learning approach. *IEEE Transactions on Vehicular Technology*, 69(11):12382–12395, 2020.
- [21] Novella Bartolini, Andrea Coletta, and Gaia Maselli. On task assignment for early target inspection in squads of aerial drones. In *2019 IEEE 39th International Conference on Distributed Computing Systems (ICDCS)*, pages 2123–2133. IEEE, 2019.
- [22] Jinyu Fu, Guanghui Sun, Jianxing Liu, Weiran Yao, and Ligang Wu. On Hierarchical Multi-UAV Dubins Traveling Salesman Problem Paths in a Complex Obstacle Environment. *IEEE Transactions on Cybernetics*, 2023.
- [23] Roberto G Ribeiro, Luciano P Cota, Thiago AM Euzébio, Jaime A Ramírez, and Frederico G Guimarães. Unmanned-aerial-vehicle routing problem with mobile charging stations for assisting search and rescue missions in postdisaster scenarios. *IEEE transactions on systems, man, and cybernetics: Systems*, 52(11):6682–6696, 2021.
- [24] Shayegan Omidshafiei, Ali-Akbar Agha-Mohammadi, Christopher Amato, Shih-Yuan Liu, Jonathan P How, and John Vian. Decentralized control of multi-robot partially observable markov decision processes using belief space macro-actions. *The International Journal of Robotics Research*, 36(2):231–258, 2017.
- [25] Chuhao Qin and Evangelos Pournaras. Coordination of drones at scale: Decentralized energy-aware swarm intelligence for spatio-temporal sensing. *Transportation Research Part C: Emerging Technologies*, 157:104387, 2023.
- [26] Mahbuba Afrin, Jiong Jin, Ashfaqur Rahman, Shi Li, Yu-Chu Tian, and Yan Li. Dynamic task allocation for robotic edge system resilience using deep reinforcement learning. *IEEE Transactions on Systems, Man, and Cybernetics: Systems*, 2023.
- [27] Chi Harold Liu, Chengzhe Piao, and Jian Tang. Energy-efficient UAV crowdsensing with multiple charging stations by deep learning. In *IEEE INFOCOM 2020-IEEE Conference on Computer Communications*, pages 199–208. IEEE, 2020.
- [28] Chenxi Zhao, Junyu Liu, Min Sheng, Wei Teng, Yang Zheng, and Jiandong Li. Multi-UAV trajectory planning for energy-efficient content coverage: A decentralized learning-based approach. *IEEE Journal on Selected Areas in Communications*, 39(10):3193–3207, 2021.
- [29] Mouna Elloumi, Riadh Dhaou, Benoit Escrig, Hanen Idoudi, and Leila Azouz Saidane. Monitoring road traffic with a UAV-based system. In *2018 IEEE Wireless Communications and Networking Conference (WCNC)*, pages 1–6. IEEE, 2018.
- [30] Hailong Huang, Andrey V Savkin, and Chao Huang. Decentralized autonomous navigation of a UAV network for road traffic monitoring. *IEEE Transactions on Aerospace and Electronic Systems*, 57(4):2558–2564, 2021.
- [31] David Castells-Graells, Christopher Salahub, and Evangelos Pournaras. On cycling risk and discomfort: urban safety mapping and bike route recommendations. *Computing*, 102:1259–1274, 2020.
- [32] Jun Tang, Songyang Lao, and Yu Wan. Systematic review of collision-avoidance approaches for unmanned aerial vehicles. *IEEE Systems Journal*, 16(3):4356–4367, 2021.
- [33] Joshua K Stolaroff, Constantine Samaras, Emma R O'Neill, Alia Lubers, Alexandra S Mitchell, and Daniel Ceperley. Energy use and life cycle greenhouse gas emissions of drones for commercial package delivery. *Nature communications*, 9(1):409, 2018.
- [34] Thomas Asikis and Evangelos Pournaras. Optimization of privacy-utility trade-offs under informational self-determination. *Future Generation Computer Systems*, 109:488–499, 2020.
- [35] John Schulman, Filip Wolski, Prafulla Dhariwal, Alec Radford, and Oleg Klimov. Proximal policy optimization algorithms, 2017.
- [36] Company DJI. DJI Phantom 4 Pro. <https://www.dji.com/uk/phantom-4-pro/info#specs>. Accessed: 2022-11-16.
- [37] Damian Wierzbicki. Multi-camera imaging system for UAV photogrammetry. *Sensors*, 18(8):2433, 2018.
- [38] Evangelos Pournaras. Multi-level reconfigurable self-organization in overlay services. 2013. Ph.D. Dissertation. TU Delft, Delft University of Technology.